JMEPEG (2016) 25:2157–2163
DOI: 10.1007/s11665-016-2057-9

1059-9495/$19.00

Bonding Interface and Bending Deformation of Al/316LSS Clad Metal Prepared by Explosive Welding

Xunzhong Guo, Minyu Fan, Liuan Wang, and Fuye Ma

(Submitted October 26, 2015; in revised form March 19, 2016; published online April 19, 2016)

The morphology, elemental distribution, and phase analysis of the bonding interface were investigated by means of SEM, EDS, and XRD to evaluate the interface bonding properties of Al/316LSS clad metal prepared by explosive welding method. Furthermore, the micro-hardness and bending properties were also investigated. The results indicated that the linear and wavy bonding interfaces coexisted and intermetallic phases were present in the local interfacial zone. Moreover, the micro-hardness value at the bonding interface with intermetallic phases was higher than that at the interface without any intermetallic phases. In addition, bulk metal compounds could easily lead to the generation of micro-cracks during the bending forming process.

Keywords Al/316LSS clad metal, bending, explosive welding, interfacial phases

1. Introduction

Double metal composites exhibit the integration and advantages of two materials. They have better overall properties than single metals and alloys and have, thus, become the hot research topic in material science (Ref 1, 2). Al/316LSS clad metal is a typical example of double metal composites. 316LSS has high strength, high hardness, and wear resistance, while aluminum has excellent plasticity, oxidation resistance, and corrosion resistance. Their composite—Al/316LSS clad metal—has been widely used in petrochemical, nuclear power, and aerospace fields because of excellent overall properties and low price (Ref 3-5).

There are several preparation methods for Al/316LSS clad metal, as described below:

(1) *Composite rolling* high-temperature isothermal rolling in the two-phase region ($\alpha + \gamma$); it is applied to billets prepared by ingot metallurgy or powder metallurgy where the strain rate is closely controlled to prevent oxidation (Ref 6). However, because it is performed isothermally followed by pack rolling to reduce the deformation resistance and improve stress states, composite rolling becomes complex and costly (Ref 6, 7).
(2) *Cast rolling process* The combination of casting and rolling process simplifies the manufacturing process, shortens the production cycle, and improves the manufacturing efficiency (Ref 8, 9). Nevertheless, the composite sheets prepared by cast rolling process have coarse microstructures and poor mechanical properties and, thus, are not suitable for engineering applications (Ref 10, 11).
(3) *Hot pressing* In this method, different foils, after cold rolling and annealing treatment, are stacked alternately and placed in the vacuum hot-pressing furnace where the ramp rate, temperature, and pressure are controlled by a computer (Ref 12). This method successfully achieves metallurgical bonding due to high-temperature inter-diffusion mechanism and super-plasticity. However, it is only suitable for fabrication of small area laminates (Ref 13).
(4) *Explosive welding* It is a promising method for the fabrication of Al/316LSS clad metal (Ref 14, 15). This method can not only achieve a metallurgical bond, but also fabricate large area laminates, which is of great technological significance (Ref 16, 17).

Al/316LSS clad metal is of fundamental importance in the aerospace industry, but only a few reports have been published on it so far. In our investigations, explosive welding method was employed to fabricate the Al/316LSS clad metal. The morphology, elemental distribution, and phase analysis of the bonding interface were investigated by means of SEM, EDS, and XRD to evaluate the interface bonding properties of the Al/316LSS clad metal. Besides, the micro-hardness and the bending properties were also investigated. The results on the fabrication of Al/316LSS clad metal have an important significance in understanding the practical fabrication and plastic forming of Al/316LSS clad metal.

2. Materials and Experimental Methods

1060 aluminum plates with dimensions of 300 mm × 350 mm × 3 mm and 316LSS plates with dimensions of 300 mm × 350 mm × 11 mm were used to prepare the Al/316LSS clad metal. The initial gap between the 316LSS layer and the aluminum layer was 0.5 mm, as shown in Fig. 1.

The assembly was fixed on a cement foundation. An iron plate of 5 mm thickness, which was used as the impact object,

Xunzhong Guo, Minyu Fan, Liuan Wang, and **Fuye Ma,** College of Material Science and Technology, Nanjing University of Aeronautics and Astronautics, Nanjing 211100, People's Republic of China. Contact e-mails: guoxunzhong@nuaa.edu.cn and mafuye@nuaa.edu.cn.

was oiled and then placed on the assembly. The distance between the iron plate and the assembly was set at 5 mm. An emulsion explosive with a density of 0.536 g/cm^3 was selected as the main component. The explosive thickness was 25 mm and detonation velocity (detonation wave speed through the explosive) was about 2600 m/s. Sodium chloride was added to the explosive to lower the detonation velocity. Electrical blasting caps were used to detonate explosives on the iron plate. Detonation waves and kinetic energy of the explosion products were transferred to the impact plate. The impact plate forced the high-speed movement of the flyer pipe towards the base pipe. Plastic deformation, local metal melting, and atomic inter-diffusion subsequently occurred at the explosive cladding interface which led to the formation of a metallurgical bond.

3. Results and Discussion

3.1 Microstructure

Three samples were cut out from the front, central, and rear positions along the detonation direction of explosives. Samples were ground and polished with a sand paper and observed under the scanning electron microscope, as shown in Fig. 2. The bonding interface at the front position along the detonation direction shows a wavy morphology whose wavelength is about 0.85 mm. Because of this wavy interface, the total bonding interface area of Al/316LSS clad metal increased, although the wavy interface is more pronounced near the explosives. It is also seen that no cracks and micro-holes form in the aluminum layer. However, some broken particles are present in the 316LSS layer. It is due to unstable energy during the initial stages and focusing large amount of energy in a small local area. Figure 2(b) shows that the bonding interface at the central position along the detonation direction also has a wavy morphology with the wavelength of 0.59 mm. The interfacial wave is obviously smaller and more disordered than that at the front position. This is because detonation energy tends to be stable when it transfers to the central position during the explosive welding. It is clear that no cracks and micro-holes form near the interface, resulting in excellent bonding between the 316LSS and aluminum layers. The bonding interface at the rear position has a linear morphology which is different from those at the other positions. This is because here the detonation energy tends to be completely stable. The white lumps with polygon or long strips that are present near the bonding interface are found to be banded structures with partial response.

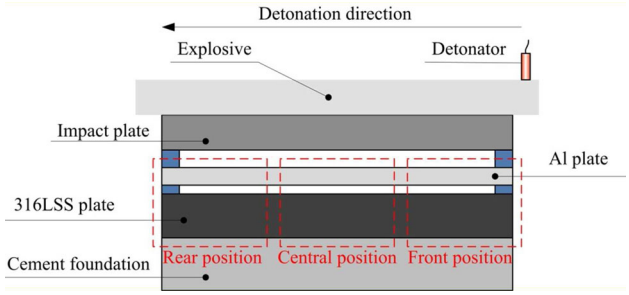

Fig. 1 Schematic showing the setup for an explosive cladding experiment of Al/316LSS clad metal

A metal particle was found in the vortex zone of the rear position and its point energy spectrum was analyzed, as shown in Fig. 3 and Table 1. Its composition was 62.15 at.% Al and 26.30 at.% Fe and it was found to be an Fe-Al intermetallic compound. After the detonation of the explosives, detonation energy transmitted to the rear position from the initiation point and tended to be steady and large. At the vortex zone, aluminum and 316LSS steels were adiabatically compressed and fast cooled, resulting in the extremely uneven local composition of the particles. Therefore, bulk intermetallic compounds formed at the local bonding interface. In addition, the phase analysis of different positions is shown in Fig. 4. The intermetallic compounds Fe_2Al_5 formed at the rear positions, corresponding to the elemental distribution of the bulk intermetallic compounds.

Figure 5 shows the distribution of different elements at the bonding interface using EDS method. The curves indicate the contents of different elements along the scanning line. The distribution of aluminum element decreases gradually from the aluminum layer to one side of the 316LSS layer at the bonding interface. Concurrently, the contents of iron, chromium, nickel, and molybdenum increase gradually from zero to a certain percentage. Hence, metallurgical bonding is observed at the bonding interface of Al/316LSS clad metal. Moreover, the thickness of the inter-diffusion layer declines gradually from the front position to the rear position along the detonation direction (10, 18, and 22 μm, respectively). This is attributed to gradual increasing detonation energy when it is transmitted along the detonation direction. The greater the detonation energy, the greater its impact load between the cladding plate and the substrate, leading to the formation of a wider bonding interface area.

3.2 Hardness Tests

The micro-hardness of the Al/316LSS clad metal was investigated by HXS-1000A micro-hardness tester with a test

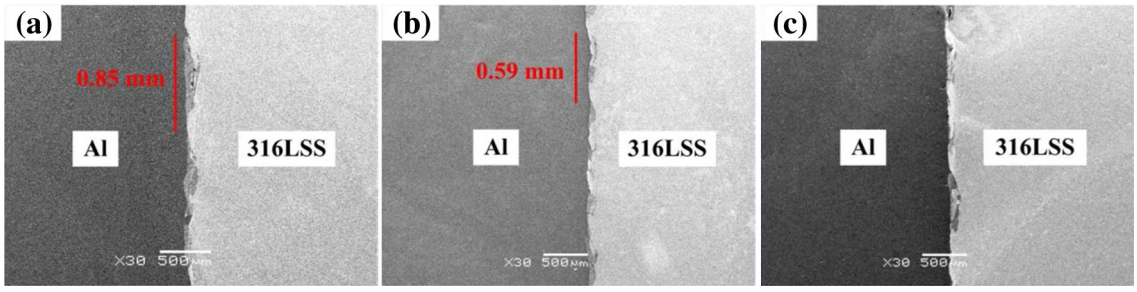

Fig. 2 Morphology of the bonding interface for Al/316LSS clad metal: (a) front position, (b) central position, and (c) rear position

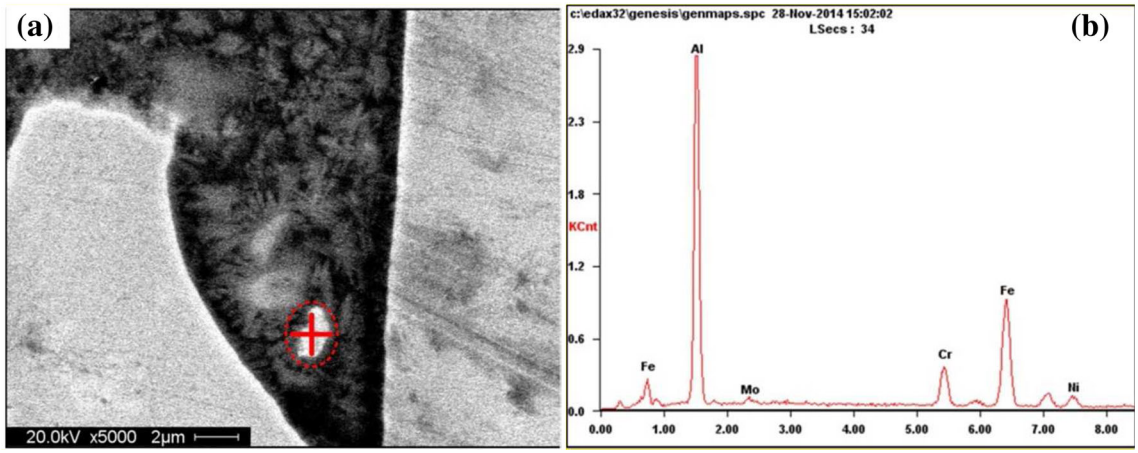

Fig. 3 Bulk intermetallic compounds: (a) location and (b) elements

Table 1 Elemental composition of bulk intermetallic compounds

Element	wt.%	at.%
AlK	44.18	62.15
MoL	01.41	00.56
CrK	09.78	07.14
FeK	38.69	26.30
NiK	05.94	03.84

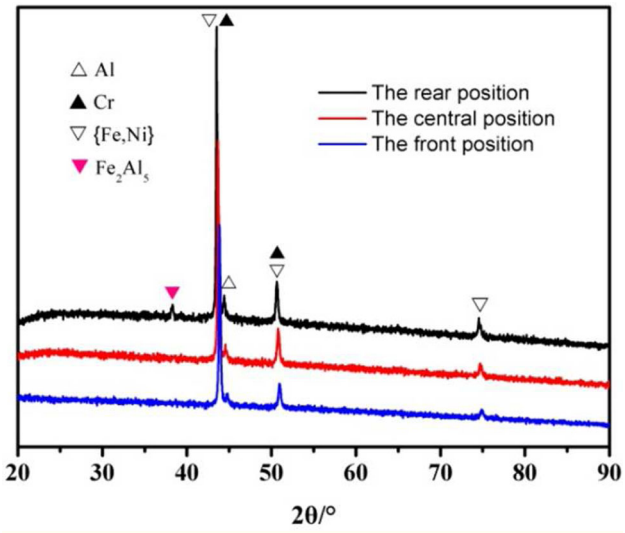

Fig. 4 Phase analysis of Al/316LSS clad metal

force of 100 g and a loading time of 15 s at an interval of 100 μm between two consecutive measured points.

The micro-hardness test indicates that the micro-hardness values of every 316LSS and aluminum layer are higher than those of the respective raw materials, while the micro-hardness value at the bonding interface is higher than those of bulk 316LSS and bulk aluminum. It is mainly due to severe plastic deformations at the wavy bonding interface and then the formation of thin metal layers near the interface during the explosive bonding process. Besides, different degrees of plastic deformations occur in the surface layers, the bottom layers, and the overall section. These deformations can not only improve the macroscopic strength of the explosive-bonded composites but also increase their micro-hardness at the respective local regions. In other words, explosive strengthening and explosive hardening of the metal matrix composites take place under an explosive load. Furthermore, from the interface to the interior of matrices, the severity of plastic deformation varies from strong to weak. As a result, the interface micro-hardness values increase significantly, much higher than those of the matrices. In addition, the hardening of the aluminum and 316LSS matrices is mainly due to the plastic deformations and the resulting work hardening, while the hardening at the bonding interface is mainly due to fibrous plastic deformations and the resulting work hardening.

Furthermore, the micro-hardness values of the bonding interface at the rear position are higher than those at the other positions. This is partly attributed to the generation of bulk intermetallic compounds at the bonding interface (Fig. 6).

3.3 Bending Deformation

In order to investigate the plastic forming ability of Al/316LSS clad metal, a three-point bending test was carried out using a SANS CMT5105 electronic universal testing machine. The bending specimen of Al/316LSS clad metal was cut at the front position without the bulk intermetallic compounds and another one at the rear position with bulk intermetallic compounds. The bending radius was 3 mm and the bending angle was calculated by measuring the displacement of the bending head. After bending of 30°, 40°, and 50°, no marco-delamination is observed at the interface of the Al/316LSS clad metal, indicating an excellent interface bonding property, as shown in Fig. 7.

3.4 Morphology

In order to evaluate the bending properties of the Al/316LSS clad metal, a scanning electron microscope (SEM) was used to observe the bending specimens cut from the front and rear positions after 30°, 40°, and 50° bending. The specimens of Al/316LSS clad metal are shown in Fig. 8 after 30° bending. It is found that no cracks form in the aluminum layers, the 316LSS

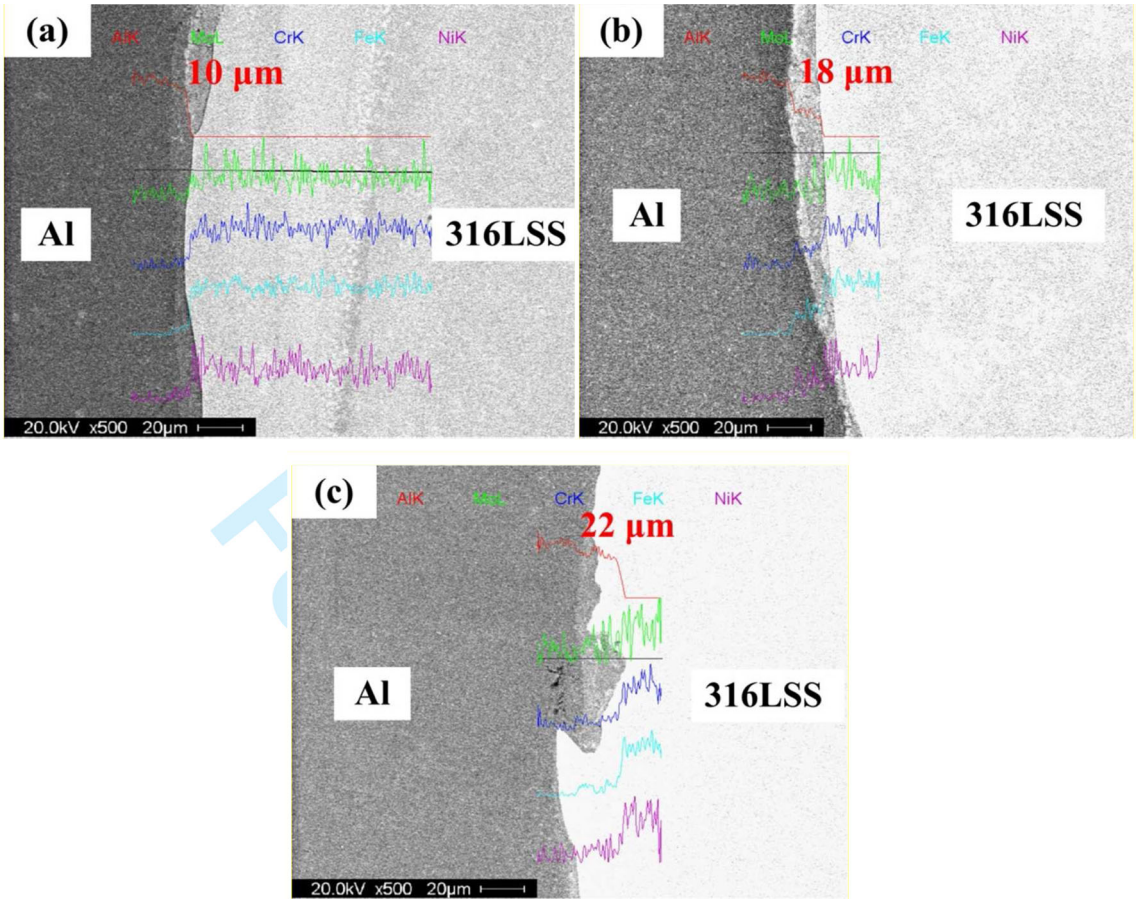

Fig. 5 Elemental distribution at the bonding interface for Al/316LSS clad metal: (a) front position, (b) central position, and (c) rear position

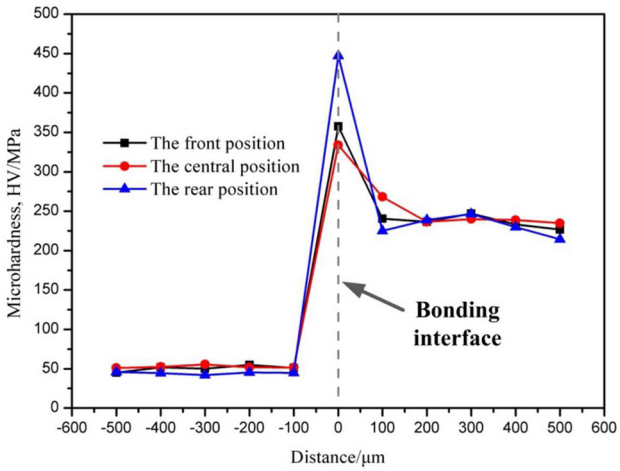

Fig. 6 The micro-hardness of Al/316LSS clad metal

layer, and the bonding interface of both the samples. Therefore, Al/316LSS clad metal can be bent to 30°.

The bending specimens of Al/316LSS clad metal are shown in Fig. 9 after 40° bending. No cracks still form in the aluminum layers, the 316LSS layer, and the bonding interface of the front position sample. However, some obvious cracks are observed at the bonding interface of the rear position sample. Furthermore, the crack growth direction is consistent with the loading direction, and the cracks extend to the 316LSS layer.

Figure 10 shows the bending specimens of Al/316LSS clad metal after 50° bending. Obviously, some cracks have formed at the bonding interface of the front position sample and extended to the 316LSS layer. Moreover, the crack growth direction is consistent with the loading direction; further, delaminations occur between the diffusion layer and 316LSS layer. Meanwhile, the diffusion layer of the rear position sample has been completely broken and is composed of many broken particles. These broken particles were found to form mainly around the bulk intermetallic compounds. As a result, the rear position with bulk intermetallic compounds can only be bent to 30°, while the front position without any bulk intermetallic compound can be bent to 40°.

There are no bulk intermetallic compounds present at the front position. The initial bending angle of the micro-cracks at the front position is higher than that at the rear position with bulk intermetallic compounds. However, micro-cracks are still mainly generated at the bonding interface of the front position. It is mainly due to the large plastic deformation variation between the aluminum layer and 315LSS layer. During the bending forming process, the coordinate deformation mainly occurred at the bonding interface and shear stress was easily generated in this region. In addition, the micro-hardness value of diffusion layer is higher than those of matrix layers, partly leading to micro-cracks at the bonding interface.

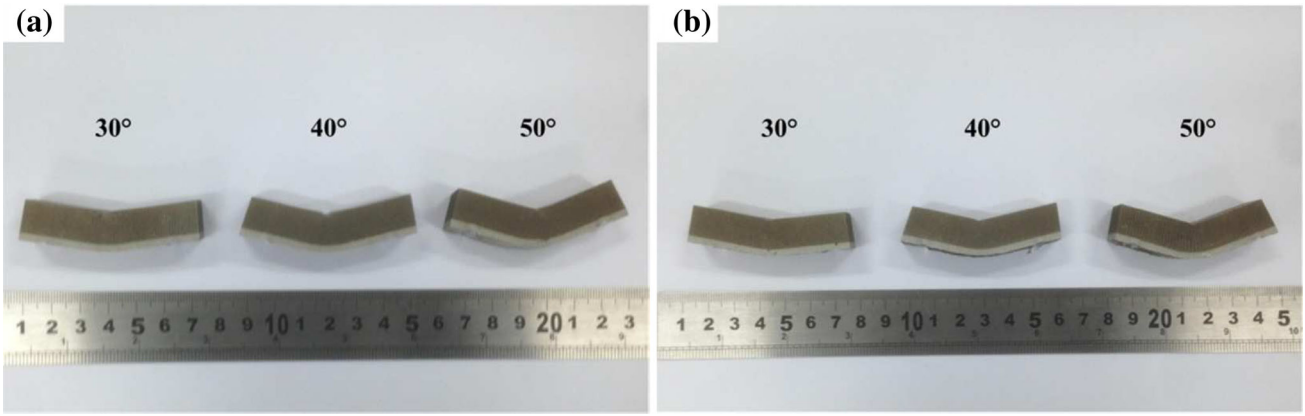

Fig. 7 Morphology of Al/316LSS clad metal after bending deformation: (a) 30°, 40°, and 50° bending (front position); (b) 30°, 40°, and 50° bending (rear position)

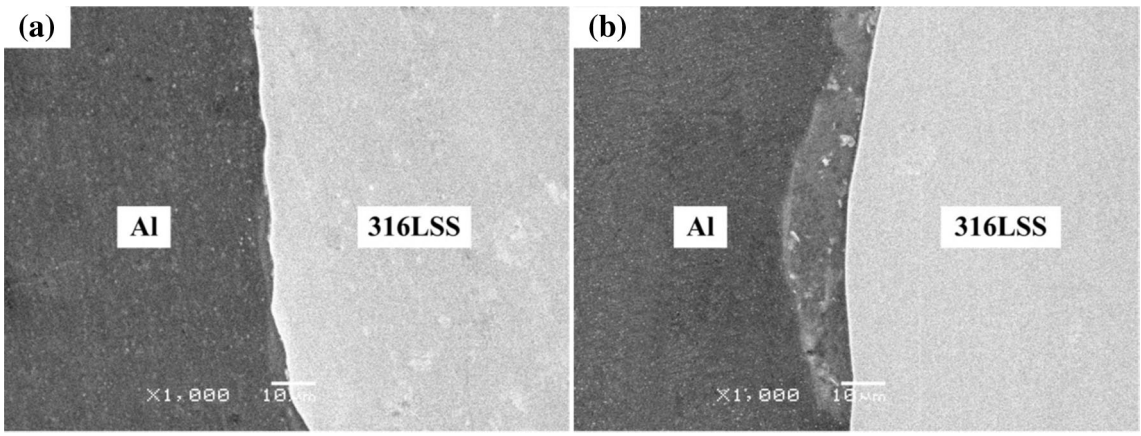

Fig. 8 Morphology of Al/316LSS clad metal after bending deformation of 30 degrees: (a) front position and (b) rear position

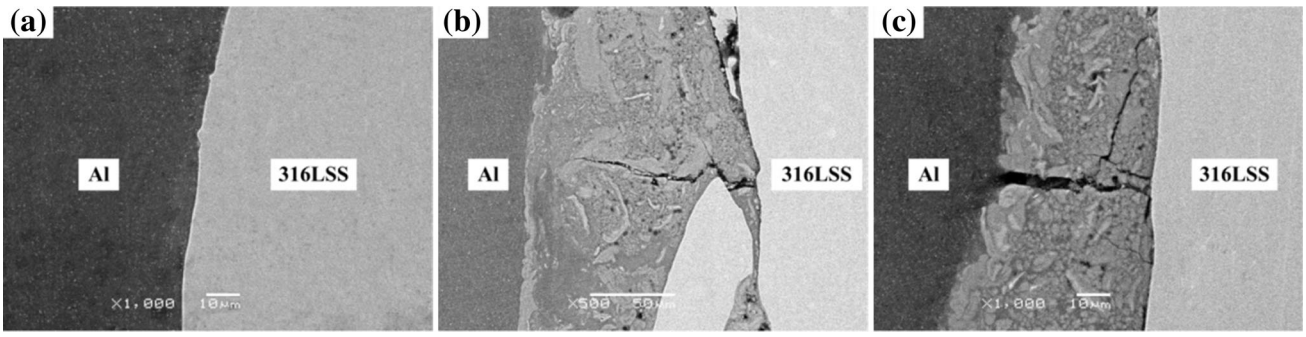

Fig. 9 Morphology of Al/316LSS clad metal after bending deformation of 40 degrees: (a) front position, (b) rear position (×500), and (c) rear position (×1000)

There are bulk intermetallic compounds present at the rear position and some obvious cracks form at the bonding interface of the rear position after 40° bending. Furthermore, micro-cracks are mainly generated at the tips of the bulk intermetallic compounds and broken particles form mainly around them. At the vortex zone, aluminum and 316LSS steels were adiabatically compressed and fast cooled, bringing about extremely uneven compositions of local metal particles. Therefore, bulk intermetallic compounds formed at the local bonding interface. When the bulk metal compounds were cooled, a stress concentration was generated, and the bulk metal compounds became the cores of the micro-cracks during the bending forming process. Hence, bulk metal compounds can easily lead to the generation of micro-cracks.

After bending deformation, micro-hardness measurements were also taken on the Al/316LSS clad metal using a Shanghai

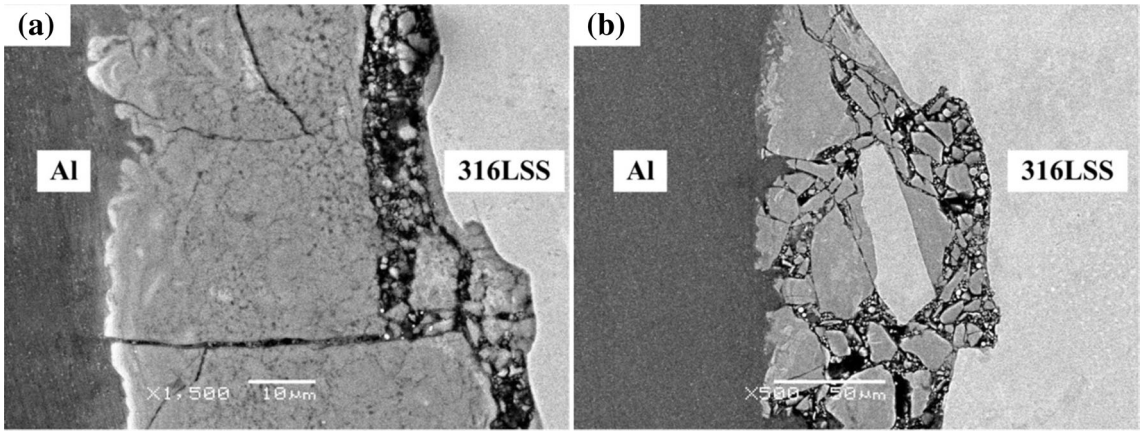

Fig. 10 Morphology of Al/316LSS clad metal after bending deformation of 50 degrees: (a) front position and (b) rear position

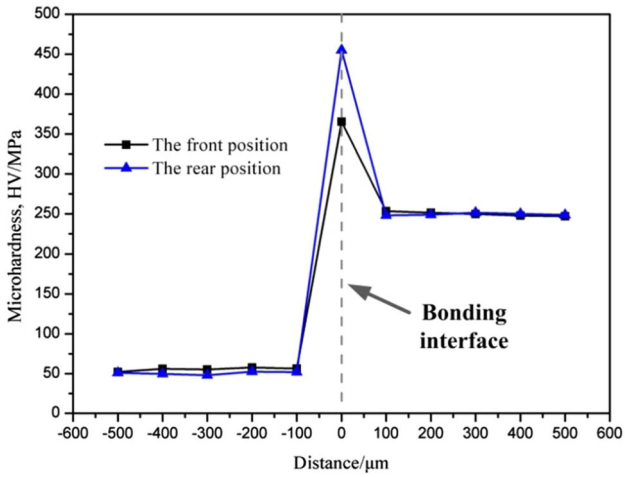

Fig. 11 Micro-hardness of Al/316LSS clad metal after bending deformation

BM HXS-1000A micro-hardness tester with an applied force of 100 g and 15 s loading time. Figure 11 shows that the micro-hardness values of the front and rear positions after bending deformation are marginally higher than those of the front and rear positions before bending deformation. It is mainly due to plastic deformations and work hardening during the bending deformation process.

4. Conclusions

(1) Explosive welding method was employed to fabricate Al/316LSS clad metal. The interface wave decreased gradually from the front position to the rear position along the detonation direction until the bonding interfaces of the rear position tended to have a linear morphology. The thickness of the inter-diffusion layer declined gradually. Moreover, bulk intermetallic compounds (Fe_2Al_5) formed at the local bonding interface of the rear position.

(2) The micro-hardness value of the bonding interface was higher than those of bulk 316LSS and bulk aluminum. Meanwhile, the micro-hardness value of the bonding interface at the rear position with bulk intermetallic compounds was higher than those at other positions.

(3) The rear position with bulk intermetallic compounds can only be bent to 30°, while the front position without any bulk intermetallic compound can be bent to 40°. The bulk metal compounds became the cores of the micro-cracks during the bending forming process. Hence, bulk metal compounds could easily lead to the generation of micro-cracks.

Acknowledgments

The present study has been supported by the National Natural Science Foundation of China (No. 51475231), the National Science Foundation of Jiangsu Province (No. SBK2015022427), the Fundamental Research Funds for the Central Universities (NO. NJ20150023), a project funded by the Priority Academic Program Development of Jiangsu Higher Education Institutions, the Foundation of Graduate Innovation Center in NUAA (kfjj20150606), and the Fundamental Research Funds for the Central Universities. The authors would like to thank Dr. Liu Peng for offering special help in the preparation of laminate materials.

References

1. Torun.O. Çelikyürek and B. Baksan, Microstructure and Strength of friction-Welded Fe-28Al and 316L Stainless Steel, *J. Mater. Sci. Eng. A*, 2011, **29–30**, p 8530–8536
2. F. Findik, Recent Developments in Explosive Welding, *J. Mater. Des.*, 2011, **32**, p 1081–1093
3. A. Almathami and M. Brochu, Microstructure and Transformation of Al-Containing Nanostructured 316L Stainless Steel Coatings Processed Using Spark Plasma Sintering, *J. Mater. Process. Technol.*, 2010, **210**(15), p 2119–2124
4. X.Z. Guo, H.B. Liu, S.Q. Cui et al., Investigation on the Maximum Thinning and Protrusion Height of the Hydroformed 316LSS/Al Clad T-Branch, *Int. J. Adv. Manuf. Technol.*, 2014, **73**(5–8), p 727–733
5. X.X. Ma, Y.D. He, D.R. Wang, and J. Zhang, Enhanced High-Temperature Corrosion Resistance of (Al_2O_3–Y_2O_3)/Pt Micro-laminated Coatings on 316L Stainless Steel Alloy, *J. Corros. Sci.*, 2012, **54**, p 183–192

6. G.P. Chaudhari and V.L. Acoff, Titanium Aluminide Sheets Made Using Roll Bonding and Reaction Annealing, *J. Intermetallics*, 2010, **18**(4), p 472–478
7. M. Ma, P. Huo, W.C. Liu et al., Microstructure and Mechanical Properties of Al/Ti/Al Laminated Composites Prepared by Roll Bonding, *J. Mater. Sci. Eng. A*, 2015, **636**, p 301–310
8. M.L. Weaver, C.W. Calhoun, and H. Garmestani, Microstructure, Texture, and Mechanical Properties of Continuously Cast Gamma TiAl, *J. Mater. Sci.*, 2002, **37**(12), p 2483–2490
9. R.I.L. Guthrie and M. Isac, Horizontal Single Belt Casting of Aluminum and Steel, *J. Steel Res. Int.*, 2014, **85**(8), p 1291–1302
10. J.W. Evans, D. Xu, and W.K. Jones, Physical and Mathematical Modeling of Metal Flow in the Continuous Casting of Steel and Aluminum, *J. Met. Mater.*, 1998, **4**(6), p 1111–1118
11. J. Sengupta, B.G. Thomas, and M.A. Wells, The Use of water Cooling During the Continuous Casting of Steel and Aluminum Alloys, *J. Metall. Mater. Trans. A*, 2005, **36**(1), p 187–204
12. Y. Sun, J. Chen, F.M. Ma et al., Tensile and Flexural Properties of Multilayered Metal/Intermetallics Composites, *J. Mater. Charact.*, 2015, **102**, p 165–172
13. M. Konieczny, Mechanical Properties of Ti-(Al_3Ti+Al) and Ti-Al_3Ti Laminated Composites, *J. Compos. Theory Pract.*, 2013, **13**(2), p 102–106
14. M. Honarpisheh, M. Asemabadi, and M. Sedighi, Investigation of Annealing Treatment on the Interfacial Properties of Explosive-Welded Al/Cu/Al Multilayer, *J. Mater. Des.*, 2012, **37**, p 122–127
15. A. Karolczuk, M. Kowalski, R. Bański et al., Fatigue Phenomena in Explosively Welded Steel–Titanium Clad Components Subjected to Push–Pull Loading, *J. Int. J. Fatigue*, 2013, **48**, p 101–108
16. M.A. Habib, H. Keno, R. Uchida et al., Cladding of Titanium and Magnesium alloy Plates Using Energy-Controlled Underwater Three Layer Explosive Welding, *J. Mater. Process. Technol.*, 2015, **217**, p 310–316
17. I.A. Bataev, A.A. Bataev, V.I. Mali et al., Structural and Mechanical Properties of Metallic-Intermetallic Laminate Composites Produced by Explosive Welding and Annealing, *J. Mater. Des.*, 2012, **35**, p 225–234